JACS
JOURNAL OF THE AMERICAN CHEMICAL SOCIETY

Article

Evidence for Modulation of Oxygen-Rebound Rate in Control of Outcome by Iron(II)- and 2-Oxoglutarate-Dependent Oxygenases

Juan Pan, Eliott S. Wenger, Megan L. Matthews, Christopher J. Pollock, Minakshi Bhardwaj, Amelia J. Kim, Benjamin D. Allen, Robert B. Grossman, Carsten Krebs, and J. Martin Bollinger, Jr.

J. Am. Chem. Soc., **Just Accepted Manuscript** • DOI: 10.1021/jacs.9b06689 • Publication Date (Web): 01 Sep 2019

is published by the American Chemical Society. 1155 Sixteenth Street N.W., Washington, DC 20036

Evidence for Modulation of Oxygen-Rebound Rate in Control of Outcome by Iron(II)- and 2-Oxoglutarate-Dependent Oxygenases

Juan Pan,[1,#] Eliott S. Wenger,[1,#] Megan L. Matthews,[1,4,#] Christopher J. Pollock,[1,5] Minakshi Bhardwaj,[3,6] Amelia J. Kim,[2] Benjamin D. Allen,[2] Robert B. Grossman,[3] Carsten Krebs,[1,2,] J. Martin Bollinger, Jr.[1,2,*]*

[1]Department of Chemistry and [2]Department of Biochemistry and Molecular Biology, The Pennsylvania State University, University Park, Pennsylvania 16802, United States

[3]Department of Chemistry, University of Kentucky, Lexington, Kentucky 40546-0312, United States

[4]Present address: Department of Chemistry, University of Pennsylvania, Philadelphia, Pennsylvania, 19104-6323, United States

[5]Present address: Cornell High Energy Synchrotron Source, Wilson Laboratory, Cornell University, Ithaca, New York 14853, United States

[6]Present address: Department of Pharmaceutical Sciences, University of Kentucky, Lexington, Kentucky 40546-0312, United States

[#]These authors contributed equally

[*]To whom correspondence should be addressed: email ckrebs@psu.edu, jmb21@psu.edu

ABSTRACT

Iron(II)- and 2-oxoglutarate-dependent (Fe/2OG) oxygenases generate iron(IV)-oxo (ferryl) intermediates that can abstract hydrogen from aliphatic carbons (R–H). Hydroxylation proceeds by coupling of the resultant substrate radical (R•) and oxygen of the Fe(III)–OH complex ("oxygen rebound"). Non-hydroxylation outcomes result from different fates of the Fe(III)–OH/R• state; for example, halogenation results from R• coupling to a halogen ligand *cis* to the hydroxide. We previously suggested that halogenases control substrate-cofactor disposition to disfavor oxygen rebound and permit halogen coupling to prevail. Here, we explored the general implication that, when a ferryl intermediate can ambiguously target two substrate carbons for different outcomes, rebound to the site capable of the alternative outcome should be slower than to the adjacent, solely hydroxylated site. We evaluated this prediction for (i) the halogenase SyrB2, which exclusively hydroxylates C5 of norvaline appended to its carrier protein but can either chlorinate or hydroxylate C4 and (ii) two bifunctional enzymes that normally hydroxylate one carbon before coupling that oxygen to a second carbon (producing an oxacycle) but can, upon encountering deuterium at the first site, hydroxylate the second site instead. In all three cases, substrate hydroxylation incorporates a greater fraction of solvent-derived oxygen at the site that can also undergo the alternative outcome than at the other site, most likely reflecting increased exchange of the initially O_2-derived oxygen ligand in the longer-lived Fe(III)–OH/R• states. Suppression of rebound may thus be generally important for non-hydroxylation outcomes by these enzymes.

INTRODUCTION

In biology, hydrogen-atom (H•) transfer (HAT) from an aliphatic carbon to an iron(IV)-oxo (ferryl) intermediate enables an array of primarily oxidative transformations for which synthetic-chemical counterparts are generally underdeveloped. Formation of a carbon-centered substrate radical (R•) can initiate stereoinversion, desaturation, C–C-bond fragmentation, ring expansion, or coupling to a heteroatom (oxygen, sulfur, or halogen) or sp^2-hybridized carbon.[1-8] The most versatile subset of enzymes with this *modus operandi* are the iron(II)- and 2-oxoglutarate-dependent (Fe/2OG) oxygenases.[1,5,9] These enzymes share a largely conserved tertiary structure, known variously as the cupin, β-sandwich, or jelly-roll fold. They are represented in all three domains of life and have crucial roles in, for example, nutrient acquisition,[10] synthesis of connective tissue,[11] regulation of gene expression and epigenetic inheritance,[12-14] and homeostasis of oxygen and body mass.[15-16] In plants, fungi, and bacteria, they are highly represented in biosynthetic pathways to bioactive natural products.[1] The hydroxylases (dioxygenases) are most prevalent, but Fe/2OG *mono*oxygenases mediate many other reactions, including halogenation, C–C and C–N desaturation, oxacyclization, endoperoxidation, C-C coupling, ring expansion and stereoinversion reactions.[1,9,17] A central question motivating research on these enzymes is how such a diverse set of outcomes can emerge from a single protein architecture. Answering this question requires delineation of the individual reaction pathways, the points at which they diverge, and the structural and dynamical features of the individual proteins that lead to a given pathway.

Important structural features and early reaction events are largely conserved across the family (**Scheme S1**). The Fe(II) cofactor is most often facially coordinated by three protein ligands – two His imidazoles and one Glu or Asp carboxylate. In the Fe/2OG halogenases, the Asp/Glu

residue is absent – Ala or Gly being present in its place – and a halide ion coordinates in place of the protein carboxylate.[18] The remaining three sites of the octahedral coordination sphere are occupied by the co-substrate, 2OG, which chelates the Fe(II) ion via its C1 carboxylate and C2 carbonyl groups, and a water molecule.[19-20] Binding of the prime substrate results in dissociation of the water ligand, creating a square-pyramidal Fe(II) center with an open coordination site.[21] The location of this site is relevant to the central question of control because, in the simplest case, it is the site to which O_2 adds to initiate the reaction and subsequently harbors the oxo ligand of the key ferryl complex. Published structures reveal that the C2 carbonyl group of 2OG is always *trans* to the Asp/Glu ligand, but there are two alternative sites for the C1 carboxylate – *trans* to either His ligand. In the more common configuration, carboxylate coordination *trans* to the C-terminal His leaves the site more proximal to the substrate vacant, and this geometry has therefore been termed "inline."[1] The less common geometry, with the 2OG C1 carboxylate *trans* to the N-terminal His ligand, has been termed "offline."[1] Addition of O_2 results in an intermediate that calculations suggest is best described as a Fe(III)-superoxo complex.[22] This intermediate has not been characterized in any Fe/2OG enzyme, but structural cognates have been detected in related enzymes.[23-24] Decarboxylation of 2OG (C1–C2 cleavage) accompanied by C2–O coupling produces an Fe(II)-peroxysuccinate complex,[22] which was recently structurally characterized in the hydroxylase, VioC.[25] This intermediate undergoes O–O-bond heterolysis to generate the succinate-coordinated ferryl complex. This sequence of steps results in incorporation of one atom of O_2 into succinate and the other into the ferryl complex, where it has been shown for the case of the dioxygenases to undergo exchange with solvent in competition with incorporation into the product.[1,26-27] Boal and co-workers proposed for the halogenases that second-sphere interactions can, even after inline addition of O_2, steer the peroxide unit of the peroxysuccinate complex so as

to locate the oxo ligand of the ferryl moiety offline.[28] Regardless of the precise sequence of steps and interactions by which the oxo might be guided to the offline position, its location there is thought to be, at least for some cases, crucial to control of the reaction outcome, as outlined below.

Pathways leading to hydroxylation, halogenation, stereoinversion, desaturation, and endoperoxidation have been partially mapped.[25,27,29-39] Each begins with HAT from the substrate carbon to the ferryl moiety.[40] The resultant state, harboring an Fe(III)–OH form of the cofactor and a substrate radical [Fe(III)–OH/R•], is thought to be the key branch point for the manifold of outcomes. In hydroxylation, the R• couples with the Fe(III)-coordinated oxygen, in what Groves called "oxygen rebound" for the case of heme-dependent oxygenases.[41] In hydroxylases that have been studied, the rebound step is sufficiently rapid to prevent accumulation of the Fe(III)–OH/R• state.[29,32,37] Its facile nature raises the question of how it is averted in reactions that require different fates of the Fe(III)–OH/R• state. Other fates of this state that have been posited and, in some cases, supported by experimental data include: (i) coupling of the radical to a ligand *cis* to the oxygen in the halogenases[18,27,42] and isopenicillin *N* synthase;[4,24] (ii) HAT to the opposite face of the R• from a tyrosine residue, completing stereoinversion in carbapenem synthase (CarC);[36,43] (iii) α-heteroatom-assisted electron transfer (ET) from the R• to the Fe(III)-OH complex in the L-arginine 4,5-desaturase, NapI,[37] and the olefin-installing decarboxylase, IsnB;[44] (iv) HAT from the carbon α to the R• to the Fe(III)-OH complex in non-native C–C desaturations catalyzed by the L-arginine 3-hydroxylase, VioC,[37] and the trifunctional hydroxylase/oxacyclase/desaturase, clavaminate synthase;[45] (v) capture of O_2 by the R• in verruculogen synthase (FtmOx1);[39,46] (vi) C–C-bond formation by addition of the R• to a sp^2-hybridized carbon of the substrate in the cyclases DabC and 2-ODD;[2-3] and (vii) sigma-bond rearrangement leading to ring expansion in deacetoxycephalosporin-C synthase (DAOCS).[47] In several cases, specific adaptations disfavoring

oxygen rebound have been proposed, but the analysis of enzyme control at this crucial branchpoint is most advanced for the case of the halogenases.

Studies on the halogenase SyrB2 suggested that it controls the disposition of the substrate relative to the *cis*-chloroferryl complex to make coupling of the R• to the chlorine more facile than oxygen rebound.[27,35,48] The initial evidence involved trends in reactivity.[27] HAT from the donor in the native substrate, the C4 methyl group of L-threonine presented by the carrier protein SyrB1 (Thr-*S*-SyrB1), to the *cis*-chloroferryl complex was found to be surprisingly slow,[34] with a rate constant 100-1000-fold less than those for the corresponding steps in the reactions of two previously studied hydroxylases.[31-32] The HAT steps in reactions with two non-native SyrB1 substrates appended by either L-aminobutyrate (Aba-*S*-SyrB1, replacing the side-chain hydroxyl of Thr-*S*-SyrB1 by hydrogen) or L-norvaline (Nva-*S*-SyrB1, extending the side chain of Aba-*S*-SyrB1 by a methylene unit) were faster by factors of 13 and 130 (respectively) than with Thr-*S*-SyrB1, and the outcome changed across this substrate series from mostly (> 95%) chlorination of Thr-*S*-SyrB1, to mixed chlorination and hydroxylation of Aba-*S*-SyrB, to mostly (~ 90%) hydroxylation of Nva-*S*-SyrB1.[27,34] The trends revealed a programmed inefficiency in the HAT step, which, it was posited, results from a rigidly enforced disposition of the native substrate and *cis*-chloroferryl complex that is suboptimal for both HAT and subsequent rebound and thereby enables coupling of the C4 radical to the *cis* chlorine to prevail. By relaxing or perturbing this rigid disposition, the substrate modifications both unleash the inherent HAT potency of the *cis*-chloroferryl complex and disable suppression of the rebound step.[27] This view has been supported by a number of subsequent experimental and computational studies.[28,35,49-50] Notably, these studies have suggested that the active-site configuration enforcing slow HAT/rebound to enable chlorine

coupling is achieved not by relocation of the substrate binding site within the conserved β-sandwich architecture but rather by use of a *cis*-chloroferryl complex with offline oxo.[28,35,49]

Additional evidence for the crucial role of substrate-intermediate disposition came from a deeper kinetic analysis of the SyrB2 reaction with site-specifically deuterium-labeled isotopologs of Nva-*S*-SyrB1.[27] The analysis revealed that the same chloroferryl complex (or complexes in rapid equilibrium) can abstract H• from either C4 or C5 (**Scheme 1**). HAT from C5 *(upper path*) is preferred by a factor of ~ 6 for both the unlabeled substrate and the substrate with deuterium at both sites (4,4,5,5,5-d_5-Nva-*S*-SyrB1), but, with deuterium only at C5 (5,5,5-d_3-Nva-*S*-SyrB1), a large primary deuterium kinetic isotope effect (D-KIE) of ~ 60 reverses the regioselectivity to favor HAT from C4 (*lower two paths*) by a factor of ~ 10. HAT from C5 is invariably followed by oxygen rebound; hydroxylation is the exclusive outcome. By contrast, the slower HAT from C4 results primarily in chlorination (favored by ~ 5:1). This correlation of HAT rate with reaction outcome – *even for adjacent carbons of the same substrate* – is among the strongest evidence that substrate-intermediate disposition controls the fate of the *cis*-Cl–Fe(III)–OH/R• branch-point intermediate.

Scheme 1. Published Kinetic Dissection of the Reaction of SyrB2 with Nva-*S*-SyrB1.[27]

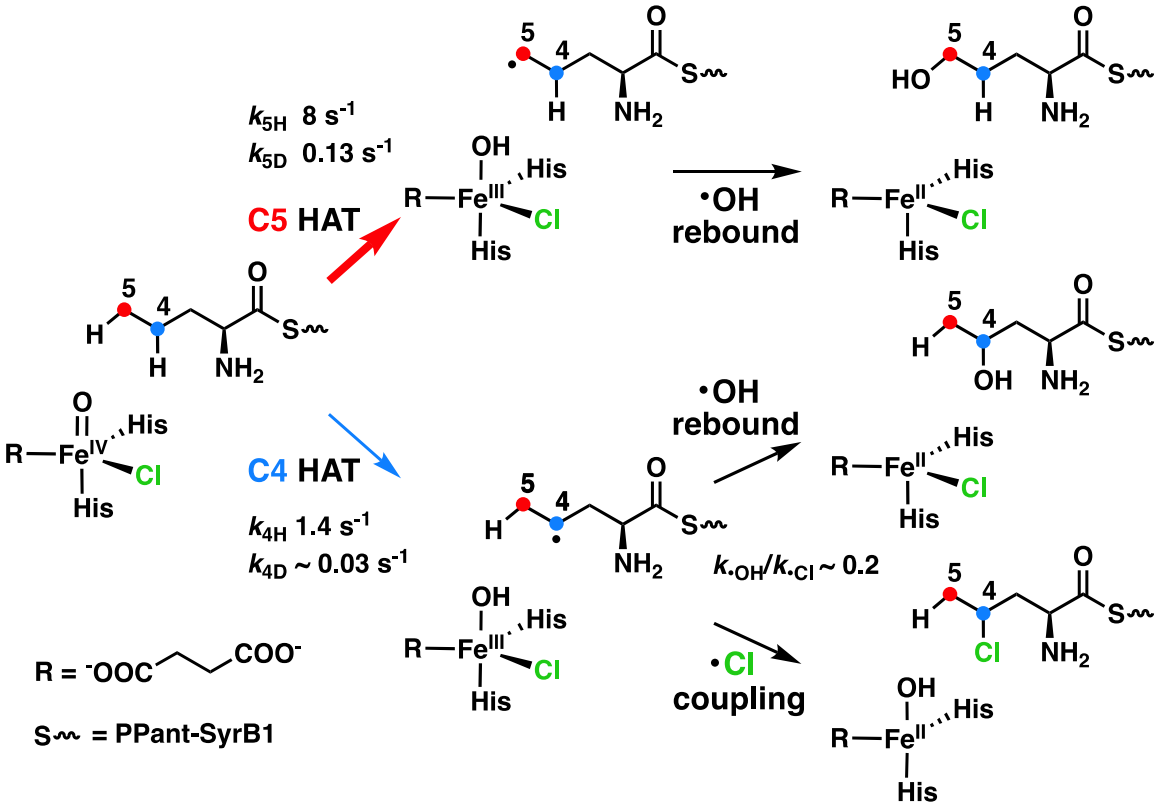

Ambiguous HAT from multiple substrate carbons and redirection by site-specific deuteration were seen before (e.g., in isopenicillin *N* synthase[4]) and have been observed since (e.g., in the L-arginine 4,5-desaturase, NapI[37]) in reactions of other mononuclear non-heme-iron enzymes. The behavior becomes evident in comparison of the kinetics of the ferryl intermediate with varied placement of deuterium in the substrate. The hallmark is that deuterium at only the preferred HAT site slows decay by less than the true, intrinsic D-KIE for the HAT step. For example, decay of the chloroferryl complex in SyrB2 with 5,5,5-d_3-Nva-*S*-SyrB1 is slower by only a factor of ~ 6 than with the unlabeled substrate. The reason is that the observed rate constant for ferryl decay in the latter case (k_{obs} ~ 9 s^{-1}) reflects the sum of the elementary rate constants for HAT from C5 (k_{5H} ~ 8 s^{-1}) and C4 (k_{4H} ~ 1.4 s^{-1}), and deuteration of only C5 diminishes only the former contribution (by the intrinsic D-KIE of ~ 60, giving k_{5D} ~ 0.13 s^{-1}), which results in k_{obs} ~

1.5 s^{-1} and an apparent D-KIE of ~ 6 (**Scheme 1**). By contrast, substitution of both positions also diminishes the contribution of HAT from C4 (k_{4D} ~ 0.03 s^{-1}), yielding k_{obs} ~ 0.16 s^{-1} and an observed D-KIE of ~ 60. Thus, an obvious manifestation of ambiguous targeting and redirection by deuterium at the preferred site is additional kinetic stabilization of the ferryl complex upon deuteration also of the secondary site.

Scheme 2. Analogous Sequences of Hydroxylation and Oxacyclization Reactions Catalyzed by LolO (**A**) and H6H (**B**)

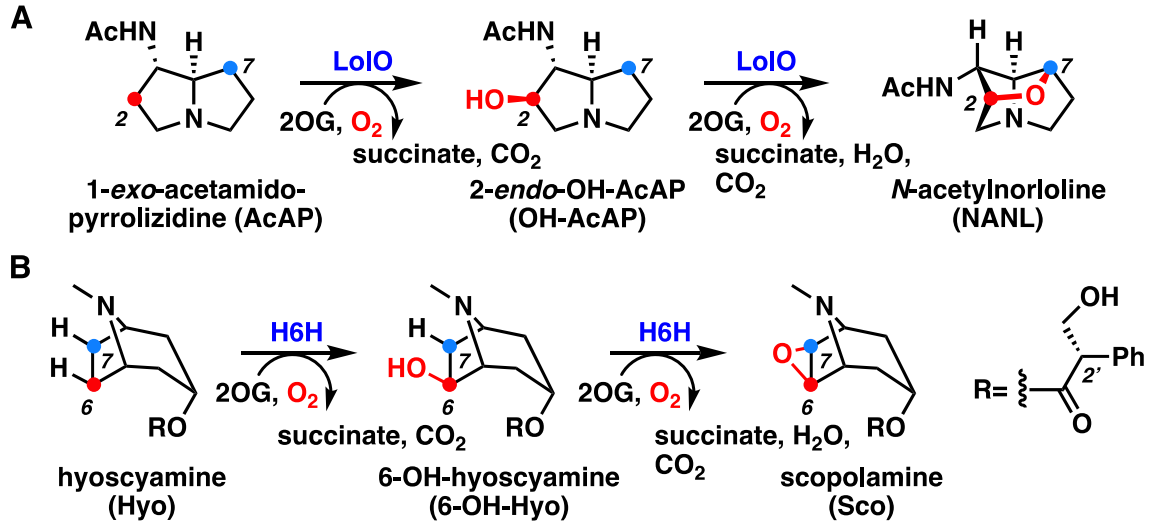

Members of a small subset of Fe/2OG oxygenases catalyze multiple reaction types in sequence. For example, fungal *N*-acetylnorloline (NANL) synthase (LolO) converts 1-*exo*-acetamidopyrrolizidine (AcAP) to its compact, tricyclic, insecticidal/anti-feedant alkaloid product by sequential hydroxylation and oxolane-forming cyclization (generally, oxacyclization) steps, each requiring an equivalent of 2OG and O_2 (**Scheme 2A**).[51-52] Analogously, hyoscyamine (Hyo) 6β-hydroxylase (H6H) from plants converts its substrate to the tropane alkaloid anesthetic drug, scopolamine (Sco), by sequential hydroxylation and epoxidation reactions (**Scheme 2B**).[53-56] These enzymes are outstanding test cases for understanding control of outcome, because each must,

in sequential steps, target different sites of the substrate for HAT and also first allow and then avert the low-barrier oxygen-rebound step. With respect to switching the site of H• abstraction, one might envisage that geometrically identical ferryl complexes would, by virtue of appropriate substrate disposition, be intrinsically competent to accept H• from either site, but with a significant bias toward the carbon that undergoes hydroxylation in the first step. In this scenario, installation of the oxygen in the first step would preclude HAT from that site in the second step (presumably, the other initially diastereotopic hydrogen on this tetrahedral carbon would be improperly disposed for HAT), causing the ferryl complex to default to the second site. One would then anticipate that site-specific deuteration of the preferred site could, as in SyrB2 with 5,5,5-d_3-Nva-*S*-SyrB1, redirect the ferryl complex to the disfavored site. In addition, HAT from the second site in the oxacyclization step should be slower than HAT from the first site in the hydroxylation step. In an alternative scenario, realignment of the substrate in the active site or formation of an alternatively configured cofactor could *more actively redirect* the second ferryl complex to the second site. With respect to averting oxygen rebound in the second step, it is not obvious, *a priori*, whether the enzymes might retard rebound, actively accelerate ring closure, or a combination of the two.

In this work, we show for both LolO and H6H that the presence of deuterium at the site normally targeted for hydroxylation does indeed redirect the ferryl complex to the site normally targeted in the second (oxacyclization) step, resulting in its hydroxylation, and we resolve rate constants for the ambiguous HAT steps. Further, we present evidence for this pair of bifunctional hydroxylase/oxacyclase enzymes that oxygen rebound to the site that can also undergo the oxacyclization outcome is retarded sufficiently that the initially O_2-derived oxygen ligand of the Fe(III)–OH/R• complex partially exchanges with solvent. Finally, we return to the previously studied case of SyrB2 with Nva-*S*-SyrB1 to obtain evidence that this same phenomenon – oxygen

exchange in the Fe(III)–OH/R• rebound state that differentially impacts the site that can also undergo the alternative outcome – is also seen in the halogenase. The conclusions imply that structurally programmed suppression of rebound may be generally important in control of outcome in the Fe/2OG-oxygenase family.

RESULTS

Evidence for modulation of rebound in the hydroxylase/oxacyclase, LolO. A recent study showed that LolO from endophytic fungi of the genus *Epichloë* catalyzes hydroxylation of AcAP at C2 followed by coupling of the nascent oxygen to C7 (**Scheme 2A**).[52] Decay of the ferryl intermediate in the hydroxylation reaction was markedly slowed by deuterium at C2 but not by deuterium at C7. A comparison of the kinetics of this ferryl complex in reactions with substrates bearing deuterium only at C2 (2,2,8-d_3-AcAP) or at both C2 and C7 (2,2,7,7,8-d_5-AcAP) (**Figure 1**) exhibits the hallmark of ambiguous ferryl targeting: the large D-KIE observed upon labeling the primary HAT site, C2, is potentiated by deuteration also of the secondary site, C7 (*compare black and green traces*). A global simulation of traces from the reactions with all four deuterium isotopologs (*solid lines*), including 7,7-d_2-AcAP (*red trace*), allowed extraction of the rate constants for decay (k_{obs}) shown in **Table 1**. For each substrate, k_{obs} is the sum of the rate constants for H(D)AT from C2 and C7 ($k_{obs} = k_2 + k_7$). These values of k_{obs} kinetically resolve ferryl decay into two parallel pathways (**Scheme 3**) and enable prediction of the product distribution for each substrate. The ~ 70-fold preference for C2 over C7 (with protium at both sites) is much greater than that for C5 over C4 in the SyrB2/Nva-*S*-SyrB1 reaction; this fact explains the more modest additional stabilization conferred by deuterium at the secondary site in the case of LolO. **Scheme 3** predicts that the ferryl complex targets C7 of 2,2,8-d_3-AcAP in ~ 35% of events [$k_{7H}/(k_{7H} + k_{2D})$

× 100%], producing the C7-hydroxylated compound (7-OH-AcAP), with a change in mass-to-charge ratio ($\Delta m/z$) of +16 (removal of protium), along with 65% [$k_{2D}/(k_{7H} + k_{2D}) \times 100\%$] of the authentic pathway intermediate, 2-*endo*-hydroxy-AcAP (2-OH-AcAP), with $\Delta m/z = +15$ (removal of deuterium). Analysis of the reaction products by LC–MS confirmed this prediction (**Figure 2A and Figure S1A**). The two products were separated chromatographically: the 2-OH-AcAP pathway intermediate elutes first at 19–20 min, and the 7-OH-AcAP compound elutes later at 21–22 min. The peak of the C7-modified product, barely visible in the chromatogram of the reaction with the unlabeled substrate, is markedly enhanced by deuterium at C2 (2,2,8-d_3-AcAP) and again suppressed when C7 is also labeled (2,2,7,7,8-d_5-AcAP). This trend in peak intensities and the $\Delta m/z$ values associated with this product (+16 with 2,2,8-d_3- and unlabeled AcAP, +15 with 2,2,7,7,8-d_5-AcAP) confirm that it is 7-OH-AcAP. In reactions with 2,2,8-d_3-AcAP in which multiple equivalents of 2OG were supplied, the early-eluting species assigned as 2-OH-AcAP could be converted to the appropriately deuterium-labeled (2,8-d_2) NANL product, with $\Delta m/z$ = +13 relative to 2,2,8-d_3-AcAP, whereas the later-eluting species assigned as 7-OH-AcAP was not further processed (**Figure S1B**). Thus, redirection of the ferryl complex to C7 by site-specific deuteration of C2 partially subverts the pathway, affording 7-OH-AcAP as a dead-end product in ~ 35%-yield.

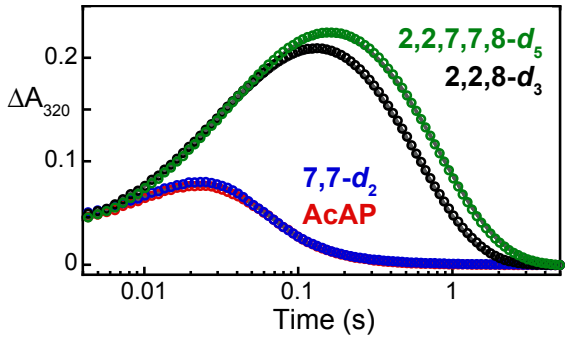

Figure 1. Kinetics of the ferryl complex, monitored by its absorbance at 320 nm, in the LolO reactions with AcAP deuterium isotopologs. An anoxic solution containing 1.1 mM LolO, 0.8 mM Fe^{II}, 5.0 mM 2OG, and 4.0 mM of the synthetic AcAP (*red*), 7,7-d_2-AcAP (*blue*), 2,2,8-d_3-AcAP (*black*), or 2,2,7,7,8-d_5-AcAP (*green*) substrate in 50 mM sodium HEPES buffer (pH 8) was mixed at 5 °C with an equal volume of the air-saturated buffer (giving ~ 0.19 mM O_2). A global simulation of the data, generated by assuming a three-state kinetic model with two irreversible steps, is shown as solid lines. Details of the analysis are provided in the *Supporting Information*. The simulation yielded a rate constant of ~ 1.2×10^5 M^{-1} s^{-1} for addition of O_2 to form the ferryl complex and the rate constants for decay of the ferryl complex (k_{obs}) by H(D)AT listed in Table 1. Note that all synthetic AcAP deuterium isotopologs are racemic; the concentrations provided are for the mixture.

Table 1. Rate Constants for Decay of the Ferryl Intermediate by H(D)AT in Hydroxylation of AcAP Deuterium Isotopologs by LolO

Substrate	k_{obs} (s^{-1})	k_{2H} (s^{-1})	k_{2D} (s^{-1})	k_{7H} (s^{-1})	k_{7D} (s^{-1})[a]
AcAP	48	47	-	0.7	-
7,7-d_2-AcAP	47	47	-	-	~ 0.03
2,2,8-d_3-AcAP	2.0	-	1.3	0.7	-
2,2,7,7,8-d_5-AcAP	1.3	-	1.3	-	~ 0.03

[a]The modest value of k_{7D} precluded its accurate determination.

Scheme 3. Kinetic Resolution of Two Possible Hydroxylations of AcAP by LolO

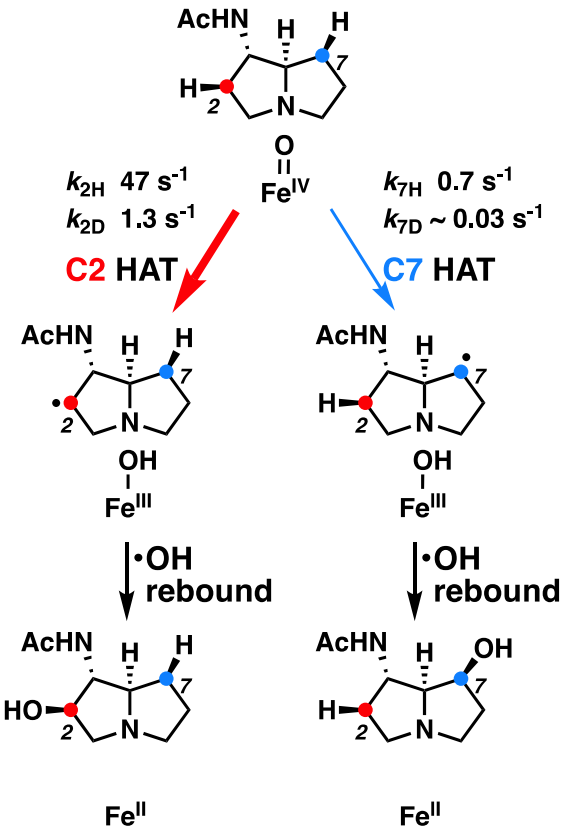

In the previous study,[52] use of $^{18}O_2$ in the LolO reaction resulted in incorporation of ^{18}O into the 2-OH-AcAP intermediate and ultimately the NANL product. With the above kinetic and LC–MS analyses revealing a small quantity of 7-OH-AcAP in the reaction with unlabeled AcAP and ~ 35% of the dead-end product in the reaction with 2,2,8-d_3-AcAP, we tested for differential ^{18}O incorporation into C2 and C7. With the unlabeled substrate, there is nearly 100% incorporation during hydroxylation of C2 (**Figure S2**): the fraction of ^{18}O in the 2-OH-AcAP (93 ± 1%) was found to be the same, within experimental error, as that in the succinate co-product (94 ± 3%), which obtains its oxygen atom from O_2 in 100% of events (with no possibility of solvent exchange) and thus provides a means to quantify contaminating atmospheric $^{16}O_2$ in the $^{18}O_2$ reaction. Although the modest yield of 7-OH-AcAP produced in this reaction (< 2%) resulted in considerable uncertainty in its measured isotopic composition, the consistently lower fraction of

^{18}O (84 ± 2%) implies 9 ± 2% solvent exchange ("washout") during C7 hydroxylation (**Figure S2**). With 2,2,8-d_3-AcAP, the lifetime of the ferryl state is enhanced by a factor of ~ 25, and, consequently, substantial washout was seen for both 2-OH-AcAP and 7-OH-AcAP products (**Figure 2B**). In this case, the isotopic compositions of both products could be precisely determined as a result of their more similar yields. Washout of the O_2-derived oxygen during hydroxylation of C7 (47.6 ± 0.4 %; *gold and orange traces*) again exceeded that during hydroxylation of C2 (40.6 ± 0.2%; *dark and light blue traces*) by ~ 7% (**Table 2**). Because this difference is modest, we verified the conclusion by also carrying out the reactions with $^{16}O_2$ in $H_2{}^{18}O$ (**Figure 2C** and **Table 3**). As expected, reactions carried out in 77% $H_2{}^{18}O$ showed greater ^{18}O incorporation into the 7-OH-AcAP product (*gold and orange traces*) than into the 2-OH-AcAP intermediate (*dark and light blue traces*), and the values mirrored those from the $^{18}O_2/H_2{}^{16}O$ experiment. The extents of exchange were consistent for all 2OG concentrations tested, thus verifying that the differential washout is an intrinsic manifestation of the reaction mechanism and independent of experimental reactant stoichiometries.

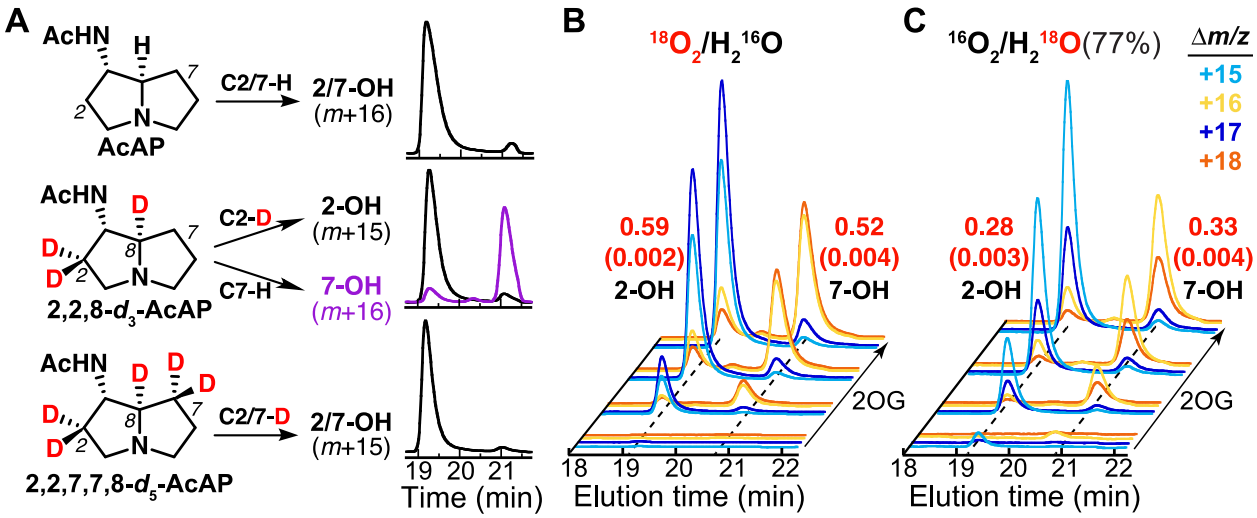

Figure 2. LC–MS characterization of the hydroxylation products in LolO reactions with AcAP deuterium isotopologs and determination of the origin of the installed oxygen atom. **(A)** Changes in mass associated with hydroxylation of the relevant isotopologs at C2 and C7 (*left*) and single-ion chromatograms (positive-ion mode) from the reactions (*right*). The trends in peak intensities and mass shift with 2,2,8-d_3-AcAP identify the first product to elute as 2-OH-AcAP and the second product to elute as 7-OH-AcAP. (**B** and **C**) Analysis by LC–MS of the differential incorporation of ^{18}O from $^{18}O_2$ (97% isotopic purity) or $H_2{}^{18}O$ (77% isotopic purity), respectively, into the C2- and C7-hydroxylation products of 2,2,8-d_3-AcAP under single-turnover conditions. Positive-mode single-ion chromatograms at the *m*/*z* values corresponding to hydroxylation with loss of deuterium and incorporation of ^{18}O (*dark blue*) or ^{16}O (*light blue*) and loss of protium with incorporation of ^{18}O (*orange*) or ^{16}O (*gold*) are shown. Reactions were carried out with limiting 2OG (0–0.8 equiv. [LolO•Fe]) and excess 2,2,8-d_3-AcAP to preclude the second (oxacyclization) step. The red values beside the traces are the fraction of ^{18}O-incorporated in the 2-OH-AcAP and 7-OH-AcAP products, with standard deviations of at least eight trials (trials with varying [2OG] were considered replicates, because this variable had no systematic effect on isotopic composition) given in parentheses. Origins of the smaller peaks are discussed in the *Supporting Information*.

Table 2. Differential **^{18}O** Incorporation at the Preferred and Alternative Positions in the LolO, H6H, and SyrB2 Reactions in **$H_2{}^{16}O$** and **$^2H_2{}^{16}O$** Solvent under **$^{18}O_2$** Gas

Enzyme	Substrate	Preferred Site Solvent Exchange (%)		Alternative Site Solvent Exchange (%)		Number of Trials
		H_2O	^2H_2O	H_2O	^2H_2O	
LolO	**AcAP**	~ 0[a]	ND[b]	9 ± 2	ND	8
LolO	**2,2,8-d_3-AcAP**	40.6 ± 0.2	28.8 ± 0.3	47.6 ± 0.4	32.8 ± 0.1	16
H6H	**Hyo**	12.5 ± 0.2	8.1 ± 0.3	66.0 ± 0.7	53.8 ± 1.7	3
H6H	**6-d_1-Hyo**	32.9 ± 0.4	24.6 ± 1.1	85.2 ± 0.3	73.7 ± 0.3	3

SyrB2	**Nva**	20	ND	50	ND	1
SyrB2	**5,5,5-d_3-Nva**	58 (58[c])	ND	69 (63[c])	ND	2

[a]Incorporation of ^{18}O in hydroxylation was not significantly different from incorporation into succinate, preventing its accurate determination
[b]Value not determined.
[c]Value when base hydrolysis was performed in 45% $H_2{}^{18}O$

Table 3. Differential ^{18}O Incorporation at the C2 and C7 Positions in the LolO Reaction with 2,2,8-d_3-AcAP in $H_2{}^{18}O$ Solvent under $^{16}O_2$ Gas[a]

	% C2 Solvent Exchange	% C7 Solvent Exchange
48% $H_2{}^{18}O$	31.5 ± 1.4	38.3 ± 1.2
77% $H_2{}^{18}O$	35.3 ± 0.3	43.5 ± 0.4

[a]The concentration of $H_2{}^{18}O$ given is the final concentration in the reaction. The observed fractional exchange has been corrected by this $H_2{}^{18}O$ isotopic purity to reflect the extent of exchange expected for 100% $H_2{}^{18}O$.

Evidence for modulation of rebound in the hydroxylase/oxacyclase, H6H. The plant Fe/2OG hydroxylase/oxacyclase, H6H, first hydroxylates C6 of Hyo and then couples the oxygen of the C6-hydroxyl group to C7 to produce the epoxide (oxirane) moiety of Sco (**Scheme 2B**). As for LolO, the presence of deuterium at C6 can redirect the hydroxylating ferryl complex to C7,[55] as confirmed by comparison of the kinetics of the ferryl state with unlabeled Hyo, 6-*exo*-d_1-hyoscyamine (6-d_1-Hyo) and 6,7-*exo*-d_2-hyoscyamine (6,7-d_2-Hyo) (**Figure 3**). Again, the significant stabilizing effect of deuterium also at the second site implies that both sites can donate H• to the same ferryl complex. Global simulation of these three traces gave the k_{obs} values for decay given in **Table 4**. Again, these values are the sums of the elementary rate constants for H(D)AT from C6 and C7 ($k_{obs} = k_6 + k_7$). These values again kinetically resolve ferryl decay into two parallel pathways (**Scheme 4**). The preference for C6 hydroxylation implied by these values (~ 30-fold) is similar to that for the case of LolO. The scheme also predicts that C7 should be

targeted in 3% of events with the unlabeled substrate and 28% of events with the 6-d_1-Hyo. Indeed, LC–MS analysis of the former reaction revealed, in addition to the major peak with $\Delta m/z = +16$ at the elution time of synthetic 6β-hydroxyhyoscyamine (6-OH-Hyo), a minor (1.5 ± 0.2 %) peak with $\Delta m/z = +16$ at the elution time of 7β-hydroxyhyoscyamine (7-OH-Hyo) (**Figure 4A** and **Table 5**). Also as predicted, the yield of the 7-OH-Hyo was markedly enhanced in the reaction with 6-d_1-Hyo but again suppressed with the substrate bearing deuterium at both sites (6,7-d_2-Hyo). In the latter case, the $\Delta m/z$ of the minor product shifted to +15, confirming that it formed by hydroxylation after removal of deuterium (from C7).

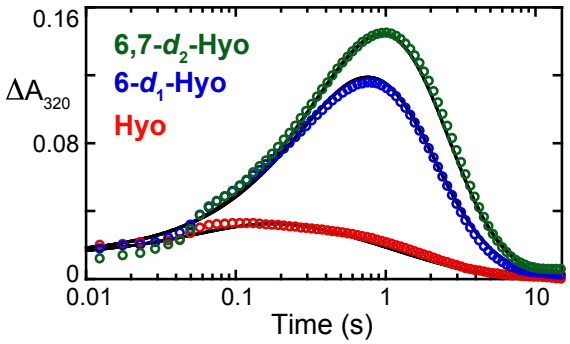

Figure 3. Kinetics of the ferryl complex, monitored by its absorbance at 320 nm, in the H6H reactions with deuterium isotopologs of Hyo. An anoxic solution containing 1.5 mM H6H, 1.2 mM Fe^{II}, 5.0 mM 2OG, and 3.0 mM of either Hyo (*red*), 6-d_1-Hyo (*blue*), or 6,7-d_2-Hyo (*green*) in 20 mM Tris-HCl, 80 mM KCl, and 10% glycerol (pH 7.5) was mixed at 5 °C with an equal volume of 50% O_2-saturated buffer (~ 0.65 mM O_2). A global simulation of the data, generated by assuming a three-state kinetic model with two irreversible steps, is shown as solid lines (see details in the *Supporting Information*). The simulation yielded a rate constant of ~ 1.1×10^3 M^{-1} s^{-1} for addition of O_2 to form the ferryl complex and the rate constants for decay of the ferryl complex (k_{obs}) by H(D)AT in Table 4.

Table 4. Rate Constants for Decay of the Ferryl Intermediate H(D)AT in Hydroxylation of the Hyoscyamine Isotopologs by H6H

Substrate	k_{obs} (s^{-1})	k_{6H} (s^{-1})	k_{6D} (s^{-1})	k_{7H} (s^{-1})	k_{7D} (s^{-1})
Hyo	15	14	-	0.5	-
6-d_1-Hyo	1.8	-	1.3	0.5	-
6,7-d_2-Hyo	1.3	-	1.3	-	~ 0.01[a]

[a]The modest value of k_{7D} precluded its accurate determination.

Scheme 4. Kinetic Resolution of Two Possible Hydroxylations of Hyoscyamine by H6H

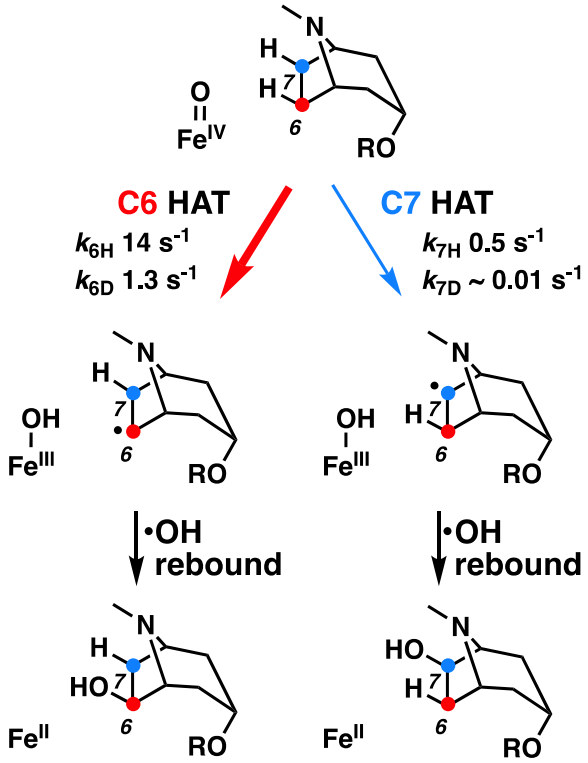

Table 5. Ratio of 6-OH-Hyo and 7-OH-Hyo formed by H6H under Single Turnover Conditions with Different Deuterium Isotopologs[a]

Substrate	% 6-OH-Hyo	% 7-OH-Hyo
Hyo	98.5 ± 0.2	1.5 ± 0.2
6-d_1-Hyo	68.6 ± 0.4	31.4 ± 0.4
6,7-d_2-Hyo	98.2 ± 0.2	1.8 ± 0.2

[a]Values were determined as the percentile of the area of each peak to the total area of the two peaks. Each value is an average of three trials.

As with LolO, analysis of reactions under $^{18}O_2$ confirmed that washout is greater for the site (C7) that undergoes the oxacyclization outcome in the second step than for the site (C6) that is programmed for hydroxylation in the first step (**Figure 4B**). For H6H, the difference is more pronounced: in the reaction with the unlabeled substrate, washout of the oxygen incorporated at C6 was modest (12 ± 0.18%), whereas washout of the oxygen incorporated at C7 was 67 ± 0.7%. In the reaction with 6-d_1-Hyo, the ~ 8-fold increased lifetime of the ferryl complex led to more washout in both products – 32.9 ± 0.4% and 85.2 ± 0.3% in the C6 and C7 products, respectively – but the relative site differential was preserved (**Table 2**).

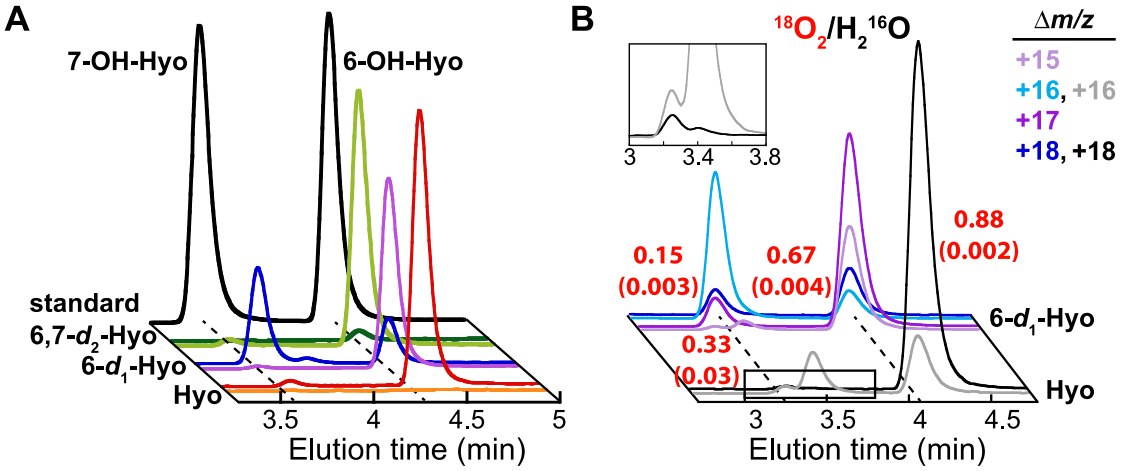

Figure 4. LC–MS characterization of the hydroxylation products in H6H reactions with Hyo deuterium isotopologs and determination of the origin of the installed oxygen atom. (**A**) Single-ion chromatograms resolving the 6-OH-Hyo and 7-OH-Hyo products. The Δ*m/z* +15 (*front*) and Δ*m/z* +16 (*back*) traces are shown for each substrate, showing hydroxylation after loss of deuterium or hydrogen, respectively. Reactions were carried out with limiting 2OG to minimize the oxacyclization reaction. (**B**) Single-ion chromatograms showing differential incorporation of ^{18}O from $^{18}O_2$ into the 6-OH-Hyo and 7-OH-Hyo products from Hyo (*front*) and 6-d_1-Hyo (*back*). Positive-mode single-ion chromatograms depicts hydroxylation products shown here as the *m/z* change (Δ*m/z*) from the substrate. For Hyo: 6-^{18}OH and 7-^{18}OH, +18 (*black*); 6-^{16}OH and 7-^{16}OH, +16 (*gray*). For 6-d_1-Hyo: 7-^{18}OH, +18 (*dark blue*, *left*); 7-^{16}OH, +16, (*light blue*, *left*); 6-^{18}OH,

+17 (*dark purple*, *right*); and 6-^{16}OH, +15 (*light purple*, *right*). The red values are the ^{18}O ratios of each product, with standard deviations from at least three trials given in parentheses. The inset is an expanded view of the boxed portion of the trace for Hyo to illustrate resolution of the 7-OH-Hyo (*leftmost gray peak*) product from the Sco product (*rightmost gray peak*) of the second (oxacyclization) reaction. Because undeuterated 7-^{16}OH-Hyo and ^{18}O-Sco have the same mass, the peak area for the former product was determined by curve fitting analysis. Origins of the peaks at $\Delta m/z$ = +18 and +16 for 6-OH-Hyo and $\Delta m/z$ = +17 for 7-OH-Hyo with the 6-d_1-Hyo substrate in Figure 4B are discussed in the *Supporting Information*.

Evidence that oxygen rebound is also slow in mixed chlorination and hydroxylation by SyrB2. In the previous study of the SyrB2 reaction with Nva-*S*-SyrB1, the C4- and C5-hydroxylated products were not chromatographically resolved, preventing assessment of the possibility that solvent exchange occurs to different extents. To assess this possibility, we developed an improved analytical method, in which the amino acid products were cleaved off the carrier protein by a brief (5 min) treatment with 0.125 M potassium hydroxide (KOH), separated by hydrophilic interaction chromatography, and detected via a prominent voltage-induced fragmentation (neutral loss of formic acid from the parent amino acid cation) in the mass spectrometer (**Figure 5A**). The reaction with the unlabeled substrate (*black*) yielded a major peak for 5-hydroxy-Nva (5-OH-Nva) eluting at ~ 4.5 min and a minor peak for 4-OH-Nva eluting at ~ 3.5 min. As expected, both reflected loss of formic acid from a parent ion with $\Delta m/z$ = +16 relative to that of Nva, corresponding to hydroxylation with removal of protium. Use of Nva-*S*-SyrB1 with deuterium at C4 (4,4-d_2-Nva-*S*-SyrB1) suppressed the earlier peak reflecting 4-hydroxylation (*red*) and enhanced the later peak reflecting 5-hydroxylation (*purple*), owing to the D-KIE on HAT from C4. The m/z values of the parent ions (see **Table S1**) and fragment ions (shown in **Figure 5A**) for the peaks established that the enhanced product formed by abstraction of protium (from C5), giving $\Delta m/z$ = +16 for the hydroxylation reaction, whereas the suppressed product resulted from abstraction of deuterium

(from C4), giving $\Delta m/z$ = +15. Use of 5,5,5-d_3-Nva-*S*-SyrB1 elicited the opposite perturbation: enhancement of the earlier peak for 4-OH-Nva (*green*) with $\Delta m/z$ of +16, reflecting hydroxylation with removal of protium from C4, and suppression of the later peak for 5-OH-Nva (*orange*), with $\Delta m/z$ of +15, reflecting hydroxylation with removal of deuterium from C5. Use of 4,4,5,5,5-d_5-Nva-*S*-SyrB1 gave a 4-OH-Nva:5-OH-Nva ratio essentially equivalent to that for the unlabeled substrate (*blue*), and, as expected, both products had $\Delta m/z$ = +15, corresponding to hydroxylation with removal of deuterium.

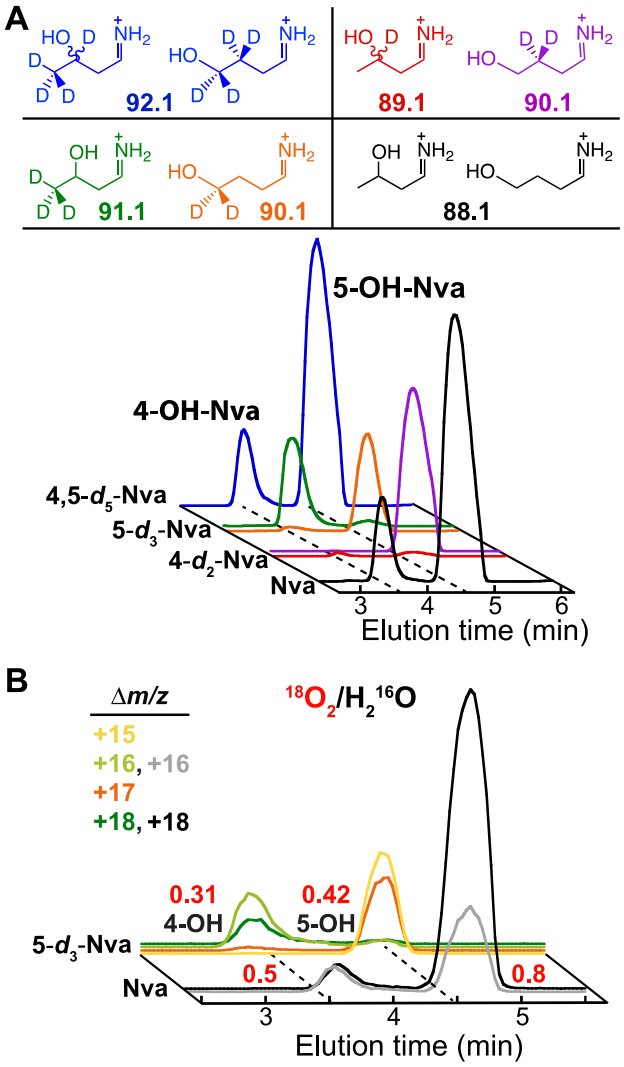

Figure 5. LC–MS characterization of the hydroxylation products in SyrB2 reactions with Nva-*S*-SyrB1 deuterium isotopologs and determination of the origin of the installed oxygen atom. **(A)** Elution profiles monitoring the daughter ions that arise from the 4-OH-Nva and 5-OH-Nva products (4-Cl-Nva product not shown) obtained in reactions of Nva-*S*-SyrB1 with deuterium isotopologs. Color-coded daughter-ion structures with *m/z* values that are associated with each elution profile are shown (*top*). Comparison of the *m*/*z* of the daughter ions from deuterated substrates to that from Nva (*m*/*z* = 88.1) permitted 4-OH-Nva and 5-OH-Nva to be distinguished both by elution time and by mass (from the number of retained deuterons). The *m/z* values for all parent cation → iminium daughter ion transitions are provided in Table S1. **(B)** Differential ^{18}O incorporation at the C4 and C5 positions in SyrB2 reactions with Nva-*S*-SyrB1 and 5,5,5-d_3-Nva-*S*-SyrB1. Chromatograms monitor the products of hydroxylation at C4 (~ 3.5 min) and C5 (~ 4.5 min). The traces are color-coded and labeled according to the Δ*m/z* relative to the substrate. The red values are the fractions of the ^{18}O-incorporated into each product.

The previous study showed that, for the reaction with 5,5,5-d_3-Nva-*S*-SyrB1, the most abundant product is 4-chloro-Nva-*S*-SyrB1.[27] For this reason, the quantities of 4-OH-Nva and 5-OH-Nva products reflected in the corresponding traces in **Figure 5A** are similar, even though C4 is the preferred HAT site with the 5,5,5-d_3-Nva-*S*-SyrB1 substrate. Because the 4-Cl-Nva product is predominant (~ 5:1 over 4-OH-Nva[27]), it was important to consider its stability to the brief base treatment used to cleave the thioester linkage to SyrB1. The reason is that, in the ^{18}O-tracer experiments, any hydrolysis of the 4-Cl-Nva product would artificially inflate the quantity of 4-OH-Nva having its alcohol oxygen derived from solvent rather than O_2, making this fraction of the product appear greater than that produced in actual hydroxylation of C4 by SyrB2. By an extended incubation of the SyrB2/5,5,5-d_3-Nva-*S*-SyrB1 reaction products in 0.25 M KOH, a base concentration twice that used in the actual product analysis, the rate constant for hydrolysis of the 4-Cl-Nva product was determined to be 0.6 ± 0.4 s^{-1} (**Figure S3A**). This result suggests that the 5-min base treatment used in the product analysis should hydrolyze ≤ 4 % of the 4-Cl-Nva primary

product, given the 2-fold lesser [KOH] used in the actual analysis and the expectation that hydrolysis should be kinetically first-order in [OH^-]. With the previously determined chlorination:hydroxylation ratio of ~ 5,[27] hydrolysis would thus diminish the *apparent* ^{18}O incorporation at C4 by, at most, a factor of 1.2 {1/[1+(0.04•5)]} from the actual fraction incorporated by authentic C4 hydroxylation.

The previous study reported that, as for native Fe/2OG dioxygenases, hydroxylation of Nva-*S*-SyrB1 by SyrB2 resulted in incorporation of ^{18}O when the reaction was carried out under an $^{18}O_2$ atmosphere. The OH-Nva product was found to have 67% ^{18}O and 33% ^{16}O, which was attributed to partial exchange of the initially O_2-derived oxygen ligand with solvent in the ferryl intermediate state. This conclusion was validated by results with 4,4,5,5,5-d_5-Nva-*S*-SyrB1: the markedly (~ 60-fold) enhanced lifetime of the ferryl complex with deuterium at both H•-donor sites resulted in 90% washout and incorporation of only ~ 10% ^{18}O. Because the 4-OH-Nva and 5-OH-Nva products were not distinguished in that study, the reported values were weighted averages for the two products. Analysis of the products from SyrB2 reactions with the Nva-*S*-SyrB1 and 5,5,5-d_3-Nva-*S*-SyrB1 substrates under $^{18}O_2$ by the new method revealed that the fractions of ^{18}O incorporated at C4 and C5 are not equivalent (**Figure 5B**). In the reaction of the unlabeled substrate, the 5-OH-Nva product contained ~ 80% ^{18}O, whereas the 4-OH-Nva contained only ~ 50% ^{18}O. These results are consistent with the site-undifferentiated value of 67% ^{18}O reported in the prior study. In the reaction with 5,5,5-d_3-Nva-*S*-SyrB1, the ~ 6-fold greater lifetime of the ferryl complex allowed for greater washout in this state, resulting in less ^{18}O incorporation at both sites. Nevertheless, the 5-OH-Nva product still had a greater fraction of ^{18}O than the 4-OH-Nva (~ 42 % compared to ~ 31 %). The ≤ 1.2-fold diminution in the apparent fraction of ^{18}O incorporated at C4 potentially caused by hydrolysis of the 4-Cl-Nva product in the

workup (as analyzed above) cannot fully account for the magnitude of this difference, consistent with the conclusion that solvent exchange also occurs in the C4-rebound state. Nevertheless, we carried out one additional control experiment in an attempt to rule out a confounding effect of 4-Cl-Nva hydrolysis on the measured O-isotope distribution of the 4-OH-Nva product. We used 0.125 M KOH quench solution prepared in 45:55 $H_2{}^{18}O$:$H_2{}^{16}O$ to liberate the products from the carrier protein (**Figure S3B**). In this workup, any hydrolysis of the chlorinated product to 4-OH-Nva would *increase* the fraction of ^{18}O in the latter product relative to the 42 % in the 5-OH-Nva product. The fraction of ^{18}O did increase, implying that some hydrolysis of the chlorinated product did indeed occur, but it was still significantly *less* (37 %) than that in the 5-OH-Nva product, which remained at 42%. The results of this control experiment thus provide both reason for caution in interpreting the apparent differential washout in the case of SyrB2 and evidence that it most likely is, as established more definitively for the hydroxylase/oxacyclase enzymes, an authentic reflection of washout in the Fe(III)–OH/R• state.

General Analysis of Solvent Exchange Rates and Mechanism(s) in the Three Enzymes. In general, branched reactions exhibit kinetic behavior that can (in our experience) confound the intuition of even an expert chemist. For this reason, and because the analysis of such reactions is at the core of this study, a brief, general tutorial is provided in the *Supporting Information*. Because incorporation of deuterium upon the H•-donating carbon(s) increases the lifetime of the ferryl complex, it necessarily leads to more exchange of the initially O_2-derived oxygen with solvent in that state, as reflected by the diminished fractions of ^{18}O from $^{18}O_2$ incorporated in the product(s) (**Table 2**). By contrast, substrate deuteration should not drastically impact the extent of washout that occurs in the Fe(III)–OH/R• state, because it should not significantly retard oxygen rebound

(or halogen coupling in SyrB2). Quantitative analysis of exchange occurring with different substrate isotopologs thus provides an independent check of the conclusion that exchange can indeed occur in the rebound state. For example, under the assumption that all exchange occurs in the ferryl state, the ~ 80% ^{18}O incorporation in the 5-OH-Nva product of SyrB2 with the unlabeled substrate would imply a ratio of HAT:exchange rates of 4:1 [4/(1+4) = 0.80], for an exchange rate constant (k_{ex}) of ~ 2 s^{-1} at 5 °C (given that k_{5H} is 8 s^{-1}). The ~ 6-fold enhancement of the ferryl lifetime with the 5,5,5-d_3-Nva-*S*-SyrB1 substrate would diminish the k_{HAT}:k_{ex} ratio to 0.67:1, giving a predicted ^{18}O incorporation of 40% in 5,5-d_2-5-OH-Nva. The agreement of this calculated value with the measured value (42%) supports the assumption that, for C5, exchange occurring in the rebound state is not a significant contributor to the total observed exchange. Application of the same analysis shows that exchange occurring only in the ferryl state cannot rationalize the data for C4. With Nva-*S*-SyrB1, the ~ 50% ^{18}O incorporation would require k_{ex} ~ 9 s^{-1} (equal to the effective rate constant for ferryl decay), inconsistent with incorporation of 80% ^{18}O at C5. Extension of the ferryl lifetime by ~ 6-fold with 5,5,5-d_3-Nva-*S*-SyrB1 should then yield only 14% ^{18}O incorporation, far less than the observed 32-37%. The explanation is that some (approximately half) of the solvent exchange reflected in the 4-OH-Nva product with unlabeled substrate occurs in the rebound state, and extension of the lifetime of the ferryl complex does not increase this contribution.

The corresponding analysis for the case of LolO is hampered somewhat by the lack of sufficient solvent exchange in hydroxylation of C2 of the unlabeled substrate for the extent of exchange to be accurately determined. However, because this fact also insures that very little exchange occurs in the Fe(III)–OH/C2• rebound state, the rate constant for exchange in the ferryl complex can be estimated from the ^{18}O incorporation at C2 in the reaction with the 2,2,8-d_3-AcAP

substrate (59%). With the k_{obs} for ferryl decay of 2.0 s^{-1}, k_{ex} must be ~ 1.4 s^{-1} to account for the observed 41% exchange. Interestingly, this value is similar to that calculated for the case of SyrB2.

The clearest evidence of solvent exchange in the rebound state comes from the fraction of ^{18}O in the 7-OH-Hyo product made by H6H. Were the observed washout to occur solely in the ferryl state, the 68% exchange seen in this product with the unlabeled substrate would require k_{ex} of > 30 s^{-1}, and the extension of the ferryl lifetime by ~ 8-fold with 6-d_1-Hyo would give ~ 95% washout, much more than the observed 82%. Here, the high extent of washout apparently results *primarily* from exchange with solvent in the rebound state.

The mechanisms of exchange of the oxygen ligand with solvent in the two states are not known, but it has been suggested (and we deem it most likely) that hydration of a stably or transiently 5-coordinate Fe center [two His imidazoles, two monodentate carboxylates (or a carboxylate and halide), and the oxygen] would be the first step for the case of the ferryl complex.[57] A similar hydration step is also proposed for the exchange observed in both heme and non-heme ferryl model complexes.[58-60] This hydration would give two ligands of equivalent redox state but different protonation states. At least one net proton transfer between these oxygen ligands, as well as some rearrangement of the coordination sphere (akin to a Berry pseudorotation), would be required to complete the net swapping of the oxo/hydroxo of the intermediate with a solvent molecule. To test the prediction that proton transfer is required for exchange, we carried out the LolO and H6H reactions in ^2H_2O and $^{18}O_2$. Solvent deuteration results in a greater fraction of ^{18}O incorporation (i.e., less exchange) into both products of both enzymes (**Figures S4–S5** and **Table 2**), consistent with the prediction that the exchange process requires at least one proton transfer. Interestingly, in both enzymes, the slowing of solvent exchange by ^2H_2O causes a leveling of the fractions of ^{18}O in the two hydroxylated products, suggesting a greater effective solvent deuterium

KIE on exchange in the rebound states than on exchange in the ferryl states. This effect provides additional corroboration that two distinct exchange processes (i.e., in both intermediate states) contribute to the overall washout, at least for the case of C7 (for both enzymes).

DISCUSSION

The conclusions from the reactivity studies on SyrB2 (i) that strict control of the disposition of the C-H bond to be cleaved relative to the *cis*-chloroferryl intermediate is necessary to allow C–Cl radical coupling to preempt oxygen rebound and (ii) that this disposition makes the preceding HAT step markedly less efficient than it would be if it were independently optimized have largely held up to subsequent experimental and computational scrutiny, but intriguing implications and follow-on questions have thus far gone unaddressed. For example, it is not known whether C–Cl coupling is, by virtue of this positioning, faster than the rebound steps of hydroxylases or, alternatively, if the rebound step becomes so sluggish that an even modestly efficient C–Cl-coupling step can prevail. Computational studies have converged on the notion that the outcome is linked to the frontier molecular orbitals (FMO) through which HAT proceeds. Rapid HAT through a σ-channel results in a HO–Fe^{III}–Cl/R• state with the radical closer to the oxygen, well poised for rebound but not for Cl• coupling. Conversely, the less efficient π-trajectory for HAT leads to a HO–Fe^{III}–Cl/R• state with the substrate radical nearly perpendicular to the HO-Fe^{III}-Cl plane and approximately equidistant from the two ligands. In this geometry, Cl• coupling can effectively compete with rebound, because it has a lower activation barrier. Splitting of the dπ* FMOs through which the alternative radical-coupling steps must proceed leads to differential overlap with the substrate p orbital, kinetically favoring Cl• coupling, despite the fact that the hydroxylation product is lower in energy.[61]

The issue can be raised, more generally, for any non-hydroxylation outcome: is the activation barrier for rebound raised, or is a still-facile rebound step preempted by an alternative process that a particular enzyme selectively promotes? In the former case, it would be important to understand whether the activation barriers of the HAT and rebound steps are inextricably coupled, as one might infer from the correlation seen for SyrB2, or whether other enzymes capable of non-hydroxylation outcomes may have evolved strategies to suppress rebound without sacrificing HAT proficiency. These issues cannot meaningfully be addressed without an experimental window to the rates of the rebound and alternative steps through which the Fe(III)-OH/R• complexes decay. Direct monitoring of these steps, of the sort presented here (and in previous work) for the ferryl-mediated HAT steps, has not been possible. The presumption has been that the substrate-radical states are kinetically masked (i.e., do not accumulate) by their relatively slow formation and fast decay (e.g., by rebound). In other systems, substrates that, upon forming radicals, react to migrate the radical (e.g., by ring opening) with known rate constants, giving characteristic products, have been used to time the rebound step. Although this "radical-clock" approach has provided important insights, it generally requires rather drastic modifications to substrates and rests on the dual assumptions that these modifications do not change the mechanism and that binding in the active site does not markedly perturb the rates of competing radical-timing steps relative to the values known in solution or the gas phase. Approaches to probe downstream steps on native substrates would, seemingly, have value.

The three systems probed in this work share the common feature of generating ferryl complexes that can ambiguously target either of two carbon centers for HAT, always hydroxylating one site but either hydroxylating or (in the proper context) mediating a different transformation of the other. In light of our expectation from previous work that prevention of

rebound is generally required to enable such alternative reactivities, we posited that quantitative comparison of exchange of the initially O_2-derived oxygen ligand with solvent (washout) during the hydroxylation sequence might reveal site-to-site differences in rebound efficiency. Whereas the washout known to occur in the ferryl complexes would necessarily diminish incorporation of ^{18}O from $^{18}O_2$ *at both sites to the same extent,* formation of a radical at two different sites could lead to different levels of exchange, assuming that either one of the pair of Fe(III)–OH/R• complexes would have a lifetime sufficient for solvent exchange to compete with rebound.

The results of this study confirm that the pair of substrate radicals formed in all three enzymes do indeed react differently in a manner that leads to differential ^{18}O incorporation/washout. We considered two possible mechanisms by which this difference could arise. In the first, which we consider less likely, hydration of the ferryl complex could give a stable complex with two coordinated oxygens – the oxo, initially derived from O_2, and a *cis*-coordinated solvent molecule. In this case, the different disposition of the two possible carbon-centered radicals could cause them to partition differently in coupling to one or the other oxygen ligand, resulting in differential incorporation of the one initially derived from O_2. Indeed, two recent studies have highlighted the potential for ferryl hydration.[57,62] Although for LolO and H6H, this hydration could even reflect the functionally-relevant capacity of the ferryl state to permit coordination of a C2- or C6-alkoxo ligand, so that, after the HAT step, C7• ↔ •O–C2/6 radical coupling could form the oxolane/oxirane,[55,63] it is not obvious why hydration of the *cis*-chloroferryl complex would occur in the halogenase, nor has such hydration ever been proposed. Moreover, whereas stable ferryl hydration would, in the absence of dynamic exchange with a larger pool of solvent, lead to a maximum of 50% overall washout (upon full equilibration of the two oxygen ligands), the 6-fold increase in the ferryl lifetime associated with use of the 5,5,5-d_3-Nva-*S*-SyrB1 substrate in the

SyrB2 reaction results in more than 50% washout at both sites, and the ~ 60-fold stabilization afforded by 4,4,5,5,5-d_5-Nva-*S*-SyrB1 allows 90% washout overall,[27] establishing that actual, dynamic exchange with a larger pool of solvent molecules must occur.

This dynamic solvent exchange of the oxygen ligand, *occurring in both the ferryl and ferric (rebound) states* (**Scheme 5**), can fully explain the differential washout. In this case, the competition between HAT and exchange in the common ferryl state and between rebound and exchange in each of the two Fe(III)–OH/R• states would determine the fraction of the ^{18}O from $^{18}O_2$ incorporated at each site. Under the additional assumption that the position of the radical should have no impact on the rate of ligand exchange with solvent in the latter intermediates, the magnitude of the difference in washout would be a function of both (i) the difference between the lifetimes of the intermediates and (ii) the relative magnitudes of the exchange and rebound rate constants. According to this interpretation, the rebound states with the radicals on C4 (for SyrB2/Nva-*S*-SyrB1) and C7 (for both LolO and H6H), which can undergo non-hydroxylation outcomes either in competition with hydroxylation (SyrB2) or in the second of the enzyme's two sequential reactions (LolO and H6H), persist longer than the corresponding states with the radical residing on the exclusively hydroxylated sites (C5 for SyrB2/Nva-*S*-SyrB1, C2 for LolO, and C6 for H6H). This correlation would suggest that retardation of oxygen rebound is a general control strategy for Fe/2OG enzymes that mediate outcomes other than hydroxylation.

Scheme 5. Schematic Representation of Solvent Exchange in the Ferryl and Fe(III)-OH States During Catalysis by the Fe/2OG Enzymes[a]

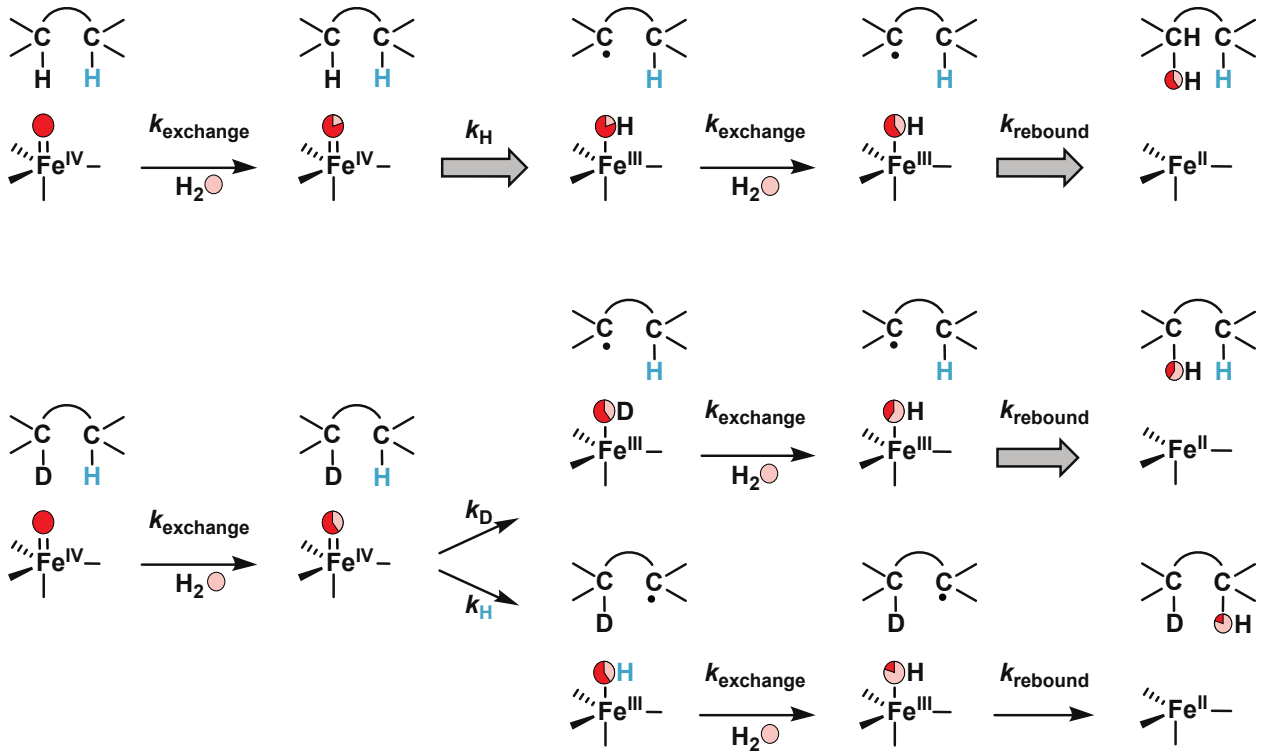

[a]We arbitrarily depict the solvent exchange steps that are followed by a "fast" decay step with 20% O-incorporation and those followed by a "slow" step with 40% O-incorporation. Fast steps are indicated by the larger gray arrows.

CONCLUSIONS

It appears that sites of substrates of Fe/2OG oxygenases that can support non-hydroxylation outcomes have rebound steps that are sufficiently sluggish to allow exchange of the hydroxo ligand with solvent to compete, implying that a structurally and dynamically programmed suppression of the default (often low-barrier) C–O-coupling step may be an important and potentially general strategy for control of outcome by the members of this versatile enzyme family. The implication that the substrate radicals on these pathways might have lifetimes sufficient for them to react with small, diffusible radical traps (including, for example, O_2) to provide further evidence for their long-lived nature remains to be explored.

ASSOCIATED CONTENT

The Supporting Information (Materials and Methods, Scheme S1, Figures S1-S12, and Tables S1-S4 in PDF format) is available free of charge on the ACS Publications website.

ACKNOWLEDGMENTS

This work was supported by the National Institutes of Health (GM113389 to C.J.P., GM113106 to J.M.B. and C.K., and GM127079 to C.K.). We thank Prof. Hung-wen Liu and Dr. Richiro Ushimaru for supplying the deuterated and hydroxylated hyoscyamine compounds and Dr. Jeffrey W. Slater for technical assistance. We dedicate this study to Larry Que, a pioneer in the field of non-heme iron chemistry, on the occasion of his 70th birthday.

REFERENCES

1. Hausinger, R. P., Fe(II)/α-ketoglutarate-dependent hydroxylases and related enzymes. *Crit. Rev. Biochem. Mol. Biol.* **2004,** *39* (1), 21-68.
2. Brunson, J. K.; McKinnie, S. M. K.; Chekan, J. R.; McCrow, J. P.; Miles, Z. D.; Bertrand, E. M.; Bielinski, V. A.; Luhavaya, H.; Oborník, M.; Smith, G. J.; Hutchins, D. A.; Allen, A. E.; Moore, B. S., Biosynthesis of the neurotoxin domoic acid in a bloom-forming diatom. *Science* **2018,** *361* (6409), 1356-1358.
3. Chang, W.-c.; Yang, Z.-J.; Tu, Y.-H.; Chien, T.-C., Reaction mechanism of a nonheme iron enzyme catalyzed oxidative cyclization via C–C bond formation. *Org. Lett.* **2019,** *21* (1), 228-232.
4. Baldwin, J. E.; Bradley, M., Isopenicillin *N* synthase: Mechanistic studies. *Chem. Rev.* **1990,** *90* (7), 1079-1088.
5. Islam, M. S.; Leissing, T. M.; Chowdhury, R.; Hopkinson, R. J.; Schofield, C. J., 2-oxoglutarate-dependent oxygenases. *Ann. Rev. Biochem.* **2018,** *87* (1), 585-620.
6. Dilley, D. R.; Wang, Z.; Kadirjan-Kalbach, D. K.; Ververidis, F.; Beaudry, R.; Padmanabhan, K., 1-Aminocyclopropane-1-carboxylic acid oxidase reaction mechanism and putative post-translational activities of the ACCO protein. *AoB Plants* **2013,** *5*, plt031.
7. Huang, X.; Groves, J. T., Oxygen activation and radical transformations in heme proteins and metalloporphyrins. *Chem. Rev.* **2018,** *118* (5), 2491-2553.
8. Kal, S.; Que, L., Jr., Dioxygen activation by nonheme iron enzymes with the 2-His-1-carboxylate facial triad that generate high-valent oxoiron oxidants. *J. Biol. Inorg. Chem.* **2017,** *22* (2-3), 339-365.
9. Bollinger, J. M., Jr.; Chang, W.-c.; Matthews, M. L.; Martinie, R. J.; Boal, A. K.; Krebs, C., Mechanisms of 2-oxoglutarate-dependent oxygenases: the hydroxylation paradigm and beyond. In *2-Oxoglutarate-Dependent Oxygenases*, Hausinger, R. P.; Schofield, C. J., Eds. Royal Society of Chemistry: London, **2015**; pp 95-122.
10. Eichhorn, E.; van der Ploeg, J. R.; Kertesz, M. A.; Leisinger, T., Characterization of α-ketoglutarate-dependent taurine dioxygenase from Escherichia coli. *J. Biol. Chem.* **1997,** *272* (37), 23031-23036.
11. Myllyharju, J., Collagen hydroxylases. In *2-Oxoglutarate-Dependent Oxygenases*, Hausinger, R. P.; Schofield, C. J., Eds. Royal Society of Chemistry: London, **2015**; pp 149-168.
12. Tsukada, Y.-i.; Fang, J.; Erdjument-Bromage, H.; Warren, M. E.; Borchers, C. H.; Tempst, P.; Zhang, Y., Histone demethylation by a family of JmjC domain-containing proteins. *Nature* **2006,** *439* (7078), 811-816.
13. Cloos, P. A. C.; Christensen, J.; Agger, K.; Maiolica, A.; Rappsilber, J.; Antal, T.; Hansen, K. H.; Helin, K., The putative oncogene GASC1 demethylates tri- and dimethylated lysine 9 on histone H3. *Nature* **2006,** *442* (7100), 307-311.
14. Klose, R. J.; Yamane, K.; Bae, Y.; Zhang, D.; Erdjument-Bromage, H.; Tempst, P.; Wong, J.; Zhang, Y., The transcriptional repressor JHDM3A demethylates trimethyl histone H3 lysine 9 and lysine 36. *Nature* **2006,** *442* (7100), 312-316.
15. Epstein, A. C. R.; Gleadle, J. M.; McNeill, L. A.; Hewitson, K. S.; O'Rourke, J.; Mole, D. R.; Mukherji, M.; Metzen, E.; Wilson, M. I.; Dhanda, A.; Tian, Y.-M.; Masson, N.; Hamilton, D. L.; Jaakkola, P.; Barstead, R.; Hodgkin, J.; Maxwell, P. H.; Pugh, C. W.; Schofield, C. J.; Ratcliffe, P. J., *C. elegans* EGL-9 and mammalian homologs define a family of dioxygenases that regulate HIF by prolyl hydroxylation. *Cell* **2001,** *107* (1), 43-54.

16. Gerken, T.; Girard, C. A.; Tung, Y. C. L.; Webby, C. J.; Saudek, V.; Hewitson, K. S.; Yeo, G. S. H.; McDonough, M. A.; Cunliffe, S.; McNeill, L. A.; Galvanovskis, J.; Rorsman, P.; Robins, P.; Prieur, X.; Coll, A. P.; Ma, M.; Jovanovic, Z.; Farooqi, I. S.; Sedgwick, B.; Barroso, I.; Lindahl, T.; Ponting, C. P.; Ashcroft, F. M.; O'Rahilly, S.; Schofield, C. J., The obesity-associated FTO gene encodes a 2-oxoglutarate-dependent nucleic acid demethylase. *Science* **2007,** *318* (5855), 1469-1472.
17. Hausinger, R. P., Biochemical diversity of 2-oxoglutarate-dependent oxygenases. In *2-Oxoglutarate-Dependent Oxygenases*, Hausinger, R. P.; Schofield, C. J., Eds. Royal Society of Chemistry: London, **2015**; pp 1-58.
18. Blasiak, L. C.; Vaillancourt, F. H.; Walsh, C. T.; Drennan, C. L., Crystal structure of the non-haem iron halogenase SyrB2 in syringomycin biosynthesis. *Nature* **2006,** *440* (7082), 368-371.
19. Que, L., Jr., One motif - many different reactions. *Nat. Struct. Biol.* **2000,** *7* (3), 182-184.
20. Koehntop, K. D.; Emerson, J. P.; Que, L., Jr., The 2-His-1-carboxylate facial triad: A versatile platform for dioxygen activation by mononuclear non-heme iron(II) enzymes. *J. Biol. Inorg. Chem.* **2005,** *10* (2), 87-93.
21. Pavel, E. G.; Zhou, J.; Busby, R. W.; Gunsior, M.; Townsend, C. A.; Solomon, E. I., Circular dichroism and magnetic circular dichroism spectroscopic studies of the non-heme ferrous active site in clavaminate synthase and its interaction with α-ketoglutarate cosubstrate. *J. Am. Chem. Soc.* **1998,** *120* (4), 743-753.
22. Ye, S. F.; Riplinger, C.; Hansen, A.; Krebs, C.; Bollinger, J. M., Jr.; Neese, F., Electronic structure analysis of the oxygen-activation mechanism by Fe-II- and alpha-ketoglutarate (alpha KG)-dependent dioxygenases. *Chem.: Eur. J.* **2012,** *18* (21), 6555-6567.
23. Mbughuni, M. M.; Chakrabarti, M.; Hayden, J. A.; Bominaar, E. L.; Hendrich, M. P.; Münck, E.; Lipscomb, J. D., Trapping and spectroscopic characterization of an Fe(III)-superoxo intermediate from a nonheme mononuclear iron-containing enzyme. *Proc. Natl. Acad. Sci., U.S.A.* **2010,** *107* (39), 16788-16793.
24. Tamanaha, E.; Zhang, B.; Guo, Y. S.; Chang, W.-c.; Barr, E. W.; Xing, G.; St Clair, J.; Ye, S. F.; Neese, F.; Bollinger, J. M., Jr.; Krebs, C., Spectroscopic evidence for the two C-H-cleaving intermediates of *Aspergillus nidulans* Isopenicillin *N* synthase. *J. Am. Chem. Soc.* **2016,** *138* (28), 8862-8874.
25. Mitchell, A. J.; Dunham, N. P.; Martinie, R. J.; Bergman, J. A.; Pollock, C. J.; Hu, K.; Allen, B. D.; Chang, W.-c.; Silakov, A.; Bollinger, J. M., Jr.; Krebs, C.; Boal, A. K., Visualizing the reaction cycle in an Iron(II)- and 2-(oxo)-glutarate-dependent hydroxylase. *J. Am. Chem. Soc.* **2017,** *139* (39), 13830-13836.
26. Chang, W.-c.; Li, J.; Lee, J. L.; Cronican, A. A.; Guo, Y., Mechanistic investigation of a non-heme iron enzyme catalyzed epoxidation in (−)-4'-methoxycyclopenin biosynthesis. *J. Am. Chem. Soc.* **2016,** *138* (33), 10390-10393.
27. Matthews, M. L.; Neumann, C. S.; Miles, L. A.; Grove, T. L.; Booker, S. J.; Krebs, C.; Walsh, C. T.; Bollinger, J. M., Jr., Substrate positioning controls the partition between halogenation and hydroxylation in the aliphatic halogenase, SyrB2. *Proc. Natl. Acad. Sci. U.S.A.* **2009,** *106* (42), 17723-17728.
28. Mitchell, A. J.; Zhu, Q.; Maggiolo, A. O.; Ananth, N. R.; Hillwig, M. L.; Liu, X. Y.; Boal, A. K., Structural basis for halogenation by iron- and 2-oxo-glutarate-dependent enzyme WelO5. *Nature chemical biology* **2016,** *12* (8), 636-640.

29. Bollinger, J. M., Jr.; Price, J. C.; Hoffart, L. M.; Barr, E. W.; Krebs, C., Mechanism of oxygen activation by taurine: α-ketoglutarate dioxygenase (TauD) from *Escherichia coli*. *Eur. J. Inorg. Chem.* **2005,** *2005*, 4245-4254.
30. Price, J. C.; Barr, E. W.; Hoffart, L. M.; Krebs, C.; Bollinger, J. M., Kinetic dissection of the catalytic mechanism of taurine:α-ketoglutarate dioxygenase (TauD) from *Escherichia coli*. *Biochemistry* **2005,** *44* (22), 8138-8147.
31. Price, J. C.; Barr, E. W.; Glass, T. E.; Krebs, C.; Bollinger, J. M., Evidence for hydrogen abstraction from C1 of taurine by the high-spin Fe(IV) intermediate detected during oxygen cctivation by taurine:α-ketoglutarate dioxygenase (TauD). *J. Am. Chem. Soc.* **2003,** *125* (43), 13008-13009.
32. Hoffart, L. M.; Barr, E. W.; Guyer, R. B.; Bollinger, J. M., Jr.; Krebs, C., Direct spectroscopic detection of a C–H-cleaving high-spin Fe(IV) complex in a prolyl-4-hydroxylase. *Proc. Natl. Acad. Sci. U.S.A.* **2006,** *103*, 14738-14743.
33. Ye, S.; Neese, F., Nonheme oxo-iron(IV) intermediates form an oxyl radical upon approaching the C–H bond activation transition state. *Proc. Natl. Acad. Sci. U.S.A.* **2011,** *108* (4), 1228-1233.
34. Matthews, M. L.; Krest, C. M.; Barr, E. W.; Vaillancourt, F. H.; Walsh, C. T.; Green, M. T.; Krebs, C.; Bollinger, J. M., Jr., Substrate-triggered formation and remarkable stability of the C–H bond-cleaving chloroferryl intermediate in the aliphatic halogenase, SyrB2. *Biochemistry* **2009,** *48* (20), 4331-4343.
35. Wong, S. D.; Srnec, M.; Matthews, M. L.; Liu, L. V.; Kwak, Y.; Park, K.; Bell, C. B.; Alp, E. E.; Zhao, J. Y.; Yoda, Y.; Kitao, S.; Seto, M.; Krebs, C.; Bollinger, J. M., Jr.; Solomon, E. I., Elucidation of the Fe(IV)=O intermediate in the catalytic cycle of the halogenase SyrB2. *Nature* **2013,** *499* (7458), 320-323.
36. Chang, W.-c.; Guo, Y.; Wang, C.; Butch, S. E.; Rosenzweig, A. C.; Boal, A. K.; Krebs, C.; Bollinger, J. M., Jr., Mechanism of the C5 stereoinversion reaction in the biosynthesis of carbapenem antibiotics. *Science* **2014,** *343* (6175), 1140-1144.
37. Dunham, N. P.; Chang, W.-c.; Mitchell, A. J.; Martinie, R. J.; Zhang, B.; Bergman, J. A.; Rajakovich, L. J.; Wang, B.; Silakov, A.; Krebs, C.; Boal, A. K.; Bollinger, J. M., Jr., Two distinct mechanisms for C–C desaturation by iron(II)- and 2-(oxo)glutarate-dependent oxygenases: importance of α-heteroatom assistance. *J. Am. Chem. Soc.* **2018,** *140* (23), 7116-7126.
38. Dunham, N. P.; Mitchell, A. J.; Del Río Pantoja, J. M.; Krebs, C.; Bollinger, J. M., Jr.; Boal, A. K., α-Amine desaturation of D-arginine by the iron(II)- and 2-(oxo)glutarate-dependent L-arginine 3-hydroxylase, VioC. *Biochemistry* **2018,** *57* (46), 6479-6488.
39. Dunham, N. P.; Del Río Pantoja, J. M.; Zhang, B.; Rajakovich, L. J.; Allen, B. D.; Krebs, C.; Bol, A. K.; Bollinger, J. M., Jr., Hydrogen donation but not abstraction by a tyrosine (Y68) during endoperoxide installation by verruculogen synthase (FtmOx1). *J. Am. Chem. Soc.* **2019,** *141* (25), 9964-9979.
40. Krebs, C.; Galonić Fujimori, D.; Walsh, C. T.; Bollinger, J. M., Jr., Non-heme Fe(IV)-oxo intermediates. *Acc. Chem. Res.* **2007,** *40* (7), 484-492.
41. Groves, J. T., Key elements of the chemistry of cytochrome P-450: the oxygen rebound mechanism. *J. Chem. Educ.* **1985,** *62* (11), 928-931.
42. Vaillancourt, F. H.; Yin, J.; Walsh, C. T., SyrB2 in syringomycin E biosynthesis is a nonheme FeII α-ketoglutarate- and O_2-dependent halogenase. *Proc. Natl. Acad. Sci. U.S.A.* **2005,** *102* (29), 10111-10116.

43. Stapon, A.; Li, R.; Townsend, C. A., Carbapenem biosynthesis: confirmation of stereochemical assignments and the role of CarC in the ring stereoinversion process from L-proline. *J. Am. Chem. Soc.* **2003,** *125* (28), 8486-8493.
44. Huang, J.-L.; Tang, Y.; Yu, C.-P.; Sanyal, D.; Jia, X.; Liu, X.; Guo, Y.; Chang, W.-c., Mechanistic investigation of oxidative decarboxylation catalyzed by two iron(II)- and 2-oxoglutarate-dependent enzymes. *Biochemistry* **2018,** *57* (12), 1838-1841.
45. Baggaley, K. H.; Brown, A. G.; Schofield, C. J., Chemistry and biosynthesis of clavulanic acid and other clavams. *Nat. Prod. Rep.* **1997,** *14* (4), 309-333.
46. Steffan, N.; Grundmann, A.; Afiyatullov, S.; Ruan, H.; Li, S.-M., FtmOx1, a non-heme Fe(II) and α-ketoglutarate-dependent dioxygenase, catalyses the endoperoxide formation of verruculogen in *Aspergillus fumigatus*. *Org. Biomol. Chem.* **2009,** *7* (19), 4082-4087.
47. Lee, H.-J.; Lloyd, M. D.; Harlos, K.; Clifton, I. J.; Baldwin, J. E.; Schofield, C. J., Kinetic and crystallographic studies on deacetoxycephalosporin C synthase (DAOCS). *J. Mol. Biol.* **2001,** *308* (5), 937-948.
48. Srnec, M.; Wong, S. D.; England, J.; Que, L., Jr.; Solomon, E. I., π-Frontier molecular orbitals in $S = 2$ ferryl species and elucidation of their contributions to reactivity. *Proc. Natl. Acad. Sci., U.S.A.* **2012,** *109* (36), 14326-14331.
49. Martinie, R. J.; Livada, J.; Chang, W.-c.; Green, M. T.; Krebs, C.; Bollinger, J. M., Jr.; Silakov, A., Experimental correlation of substrate position with reaction outcome in the aliphatic halogenase, SyrB2. *J. Am. Chem. Soc.* **2015,** *137*, 6912-6919.
50. Srnec, M.; Wong, S. D.; Matthews, M. L.; Krebs, C.; Bollinger, J. M., Jr.; Solomon, E. I., Electronic structure of the ferryl intermediate in the α-ketoglutarate dependent non-heme iron halogenase SyrB2: contributions to H atom abstraction reactivity. *J. Am. Chem. Soc.* **2016,** *138* (15), 5110-5122.
51. Pan, J.; Bhardwaj, M.; Faulkner, J. R.; Nagabhyru, P.; Charlton, N. D.; Higashi, R. M.; Miller, A.-F.; Young, C. A.; Grossman, R. B.; Schardl, C. L., Ether bridge formation in loline alkaloid biosynthesis. *Phytochemistry* **2014,** *98*, 60-68.
52. Pan, J.; Bhardwaj, M.; Zhang, B.; Chang, W.-c.; Schardl, C. L.; Krebs, C.; Grossman, R. B.; Bollinger, J. M., Jr., Installation of the ether bridge of lolines by the iron- and 2-oxoglutarate-dependent oxygenase, LolO: regio- and stereochemistry of sequential hydroxylation and oxacyclization reactions. *Biochemistry* **2018,** *57* (14), 2074-2083.
53. Li, J.; van Belkum, M. J.; Vederas, J. C., Functional characterization of recombinant hyoscyamine 6*β*-hydroxylase from *Atropa belladonna*. *Bioorg. Med. Chem.* **2012,** *20* (14), 4356-4363.
54. Ushimaru, R.; Ruszczycky, M. W.; Chang, W.-c.; Yan, F.; Liu, Y.-n.; Liu, H.-w., Substrate conformation correlates with the outcome of hyoscyamine 6*β*-hydroxylase catalyzed oxidation reactions. *J. Am. Chem. Soc.* **2018,** *140* (24), 7433-7436.
55. Ushimaru, R.; Ruszczycky, M. W.; Liu, H.-w., Changes in regioselectivity of H atom abstraction during the hydroxylation and cyclization reactions catalyzed by hyoscyamine 6*β*-hydroxylase. *J. Am. Chem. Soc.* **2019,** *141* (2), 1062-1066.
56. Hashimoto, T.; Yamada, Y., Purification and characterization of hyoscyamine 6*β*-hydroxylase from root cultures of *Hyoscyamus niger* L. *Eur. J. Biochem.* **1987,** *164* (2), 277-285.
57. Song, X.; Lu, J.; Lai, W., Mechanistic insights into dioxygen activation, oxygen atom exchange and substrate epoxidation by AsqJ dioxygenase from quantum mechanical/molecular mechanical calculations. *Phys. Chem. Chem. Phys.* **2017,** *19* (30), 20188-20197.

58. Bernadou, J.; Fabiano, A.-S.; Robert, A.; Meunier, B., "Redox tautomerism" in high-valent metal-oxo-aquo complexes. Origin of the oxygen atom in epoxidation reactions catalyzed by water-soluble metalloporphyrins. *J. Am. Chem. Soc.* **1994,** *116* (20), 9375-9376.
59. Puri, M.; Company, A.; Sabenya, G.; Costas, M.; Que, L., Oxygen atom exchange between H_2O and non-heme oxoiron(IV) complexes: ligand dependence and mechanism. *Inorg. Chem.* **2016,** *55* (12), 5818-5827.
60. Seo, M. S.; In, J.-H.; Kim, S. O.; Oh, N. Y.; Hong, J.; Kim, J.; Que Jr., L.; Nam, W., Direct evidence for oxygen-atom exchange between nonheme oxoiron(IV) complexes and isotopically labeled water. *Angew. Chem. Int. Ed.* **2004,** *43* (18), 2417-2420.
61. Srnec, M.; Solomon, E. I., Frontier molecular orbital contributions to chlorination versus hydroxylation selectivity in the non-heme iron halogenase SyrB2. *J. Am. Chem. Soc.* **2017,** *139* (6), 2396-2407.
62. Xue, J.; Lu, J.; Lai, W., Mechanistic insights into a non-heme 2-oxoglutarate-dependent ethylene-forming enzyme: selectivity of ethylene-formation versusl-Arg hydroxylation. *Phys. Chem. Chem. Phys.* **2019,** *21* (19), 9957-9968.
63. Pangia, T. M.; Yadav, V.; Gérard, E. F.; Lin, Y.-T.; de Visser, S. P.; Jameson, G. N. L.; Goldberg, D. P., Mechanistic investigation of oxygen rebound in a mononuclear nonheme iron complex. *Inorg. Chem.* **2019,** *58* (15), 9557-9561.

TOC graphic